S10

ON THE USE OF THE ANT COLONY SYSTEM FOR RADIATIVE PROPERTIES ESTIMATION

R. P. SOUTO[1], S. STEPHANY[1], J. C. BECCENERI[1], H. F. CAMPOS VELHO[1] and A. J. SILVA NETO[2],
[1] *Instituto Nacional de Pesquisas Espaciais, Av. dos Astronautas 1758, CEP 12227-010,
São José dos Campos, SP, Brazil.*
e-mail: {roberto, stephan, becce, haroldo}@lac.inpe.br
[2] *Instituto Politécnico, IPRJ, Universidade do Estado do Rio de Janeiro, UERJ,
P.O. Box 97282, 28601-970, Nova Friburgo, RJ, Brazil.*
e-mail: ajsneto@iprj.uerj.br

Abstract - An Ant Colony System (ACS) minimizer is implemented for the solution of the inverse radiative transfer problem associated to the estimation of the optical thickness, single scattering albedo and boundary surfaces diffuse reflectivities in a one-dimensional homogeneous medium. The ACS minimizer was implemented in a PC cluster using the MPI library yielding good speed-up and efficiency results. A hybridization of the ACS with the Levenberg- Marquardt method (LM) was also very effective in reducing the computational cost. The ACS minimizer and the hybridization ACS-LM are described, and test case results are discussed for both methods.

1. INTRODUCTION

Inverse radiative heat transfer problems have several relevant applications in many different areas such as astronomy, environmental sciences, engineering and medicine [7, 8, 11, 13, 17]. Some outstanding examples are parameter and function estimation for global climate models, hydrologic optics, and computerized tomography [1, 4, 5, 10, 12, 26].

When formulated implicitly [18], inverse problems are usually written as optimization problems. Several heuristics that mimic natural behaviors have been proposed for the solution of optimization problems. In particular some of the most recent algorithms, classified within the field of swarm intelligence [3], are based on the observation of social insects behaviour.

In the last decade of the past century the Ant Colony System (ACS) was applied successfully for the solution of combinatorial optimization problems [9], and more recently it has been proposed for the solution of some specific inverse problems associated to the estimation of real-valued parameters [2, 16, 24].

In the present work is presented the application of ACS for the solution of an inverse radiative transfer problem in which we seek to determine the optical thickness, the single scattering albedo and the diffuse reflectivities at the inner side of the boundaries of a one-dimensional participating medium. As experimental data we consider the intensity of the emerging radiation measured at the boundary surfaces of the medium using only external detectors.

Results for a hybridization of ACS with a deterministic gradient based method, the Levenberg-Marquardt method (LM), are also presented. The use of parallel computing in the computational implementation of the ACS is also briefly discussed.

2. MATHEMATICAL FORMULATION OF THE DIRECT AND INVERSE RADIATIVE TRANSFER PROBLEMS

2.1 Direct Problem

In Figure 1 is represented a one-dimensional, gray, homogeneous, isotropically scattering participating medium, of optical thickness τ_0 whose boundaries reflect diffusely the radiation that comes from the interior of the medium. The boundary surfaces at $\tau = 0$ and $\tau = \tau_0$ are subjected to the incidence of radiation originated at external sources with intensities A_1 and A_2, respectively.

The mathematical model for the interaction of the radiation with the participating medium is given by the linear version of the Boltzmann equation [14],

$$\mu \frac{\partial I(\tau,\mu)}{\partial \tau} + I(\tau,\mu) = \frac{\omega}{2} \int_{-1}^{1} I(\tau,\mu')\, d\mu' \qquad 0 < \tau < \tau_0,\ -1 \le \mu \le 1 \qquad (1a)$$

$$I(0,\mu) = A_1(\mu) + 2\rho_1 \int_{0}^{1} I(0,-\mu')\,\mu'\, d\mu', \qquad \mu > 0 \qquad (1b)$$

$$I(\tau_0, -\mu) = A_2(\mu) + 2\rho_2 \int_0^1 I(\tau_0, \mu') \, \mu' \, d\mu', \qquad \mu < 0 \qquad (1c)$$

where I represents the radiation intensity, τ is the optical variable, μ is the cosine of the polar angle, i.e. the angle formed between the radiation beam and the positive τ axis, ω is the single scattering albedo, and ρ_1 and ρ_2 are the diffuse reflectivities at the inner part of the boundary surfaces at $\tau = 0$ and $\tau = \tau_0$, respectively. The other symbols have already been defined.
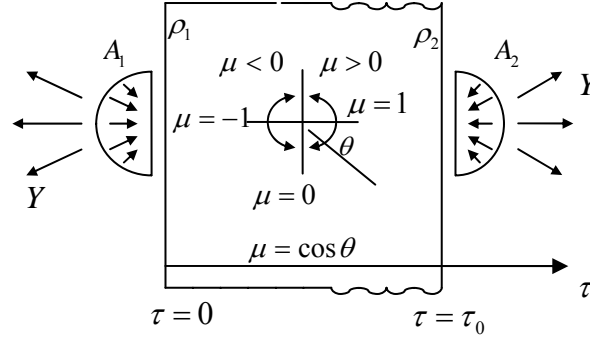

Figure 1. Schematical representation of a one-dimensional participating medium subjected to the incidence of radiation originating at external sources. Y represents the intensity of the radiation that comes out from the medium and may be measured by external detectors.

When the geometry, the boundary conditions, and the radiative properties are known, problem (1) may be solved and the radiation intensity I determined for the whole spatial and angular domains, i.e. $0 \le \tau \le \tau_0$, and $-1 \le \mu \le 1$. This is the so called direct problem.

In order to solve problem (1), we use Chandrasekhar's discrete ordinates method [6] in which the polar angle domain is discretized as represented in Figure 2, and the integral term (in-scattering) on the right hand side of eqn. (1a) is replaced by a Gaussian quadrature.

We then used a finite-difference approximation for the terms on the left hand side of eqn. (1a), and by performing forward and backward sweeps, from $\tau = 0$ to $\tau = \tau_0$ and from $\tau = \tau_0$ to $\tau = 0$, respectively, $I(\tau, \mu)$ is determined for all spatial and angular nodes of the discretized computational domain.
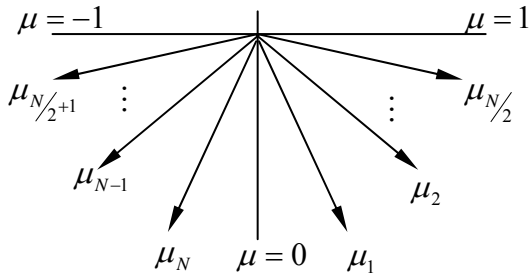

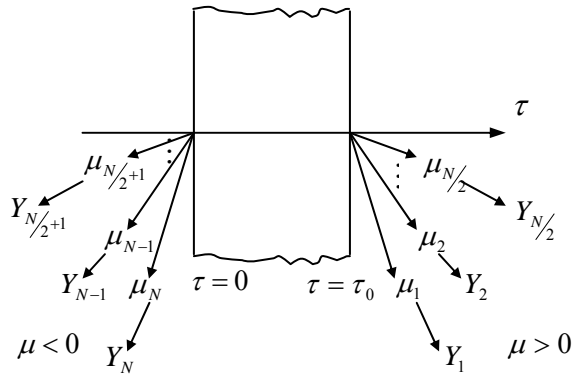Figure 2. Discretization of the polar angle domain.

Figure 3. Schematical representation of the experimental data Y_i, $i = 1,2,...,N/2$ acquired at $\tau = \tau_0$, and Y_i, $i = N/2 + 1$, $N/2 + 2,...,N$ acquired at $\tau = 0$.

2.2 Inverse Problem
We now consider that the following vector of radiative properties is unknown

$$\vec{Z} = \{\tau_0, \omega, \rho_1, \rho_2\}^T \qquad (2)$$

but experimental data on the intensity of the radiation that leaves the medium is available, i.e. Y_i, $i = 1,2,...,N$.

As schematically represented in Figure 3, half of the data is acquired at the boundary $\tau = 0$, and half at $\tau = \tau_0$, using only external detectors.

From the experimental data available, we then try to obtain estimates for the unknown radiative properties. This is the inverse radiative transfer problem we want to solve.

As the number of experimental data, N, is usually larger than the number of unknowns, we may formulate the inverse problem as a finite dimensional optimization problem in which we seek to minimize the cost function (also known as objective function) given by the summation of the squared residues between calculated and measured values of the radiation intensity,

$$Q(\vec{Z}) = \sum_{i=1}^{N} \left[I_{calc_i}(\tau_0, \omega, \rho_1, \rho_2) - Y_i \right]^2 \tag{3}$$

For the solution of the inverse problem described here, we have used a stochastic method, the Ant Colony System (ACS) as well as a hybridization of the ACS with the deterministic Levenberg-Marquardt method (ACS-LM).

3. THE ANT COLONY SYSTEM

The Ant Colony System (ACS) is a method that employs a metaheuristic based on the collective behaviour of ants choosing a path between the nest and the food source [9]. Each ant marks its path with an amount of pheromone, and the marked path is further employed by other ants as a reference. As an example of this, the sequence in Figure 4 shows how ants, trying to go from point A to point E (Figure 4a), behave when an obstacle is put in the middle of the original path, blocking the flow of the ants between points B and D (Figure 4b). Two new paths are then possible, either going to the left of the obstacle (point H) or to the right (point C). The shortest path causes a greater amount of pheromone to be deposited by the preceding ants and thus more and more ants choose this path (Figure 4c).
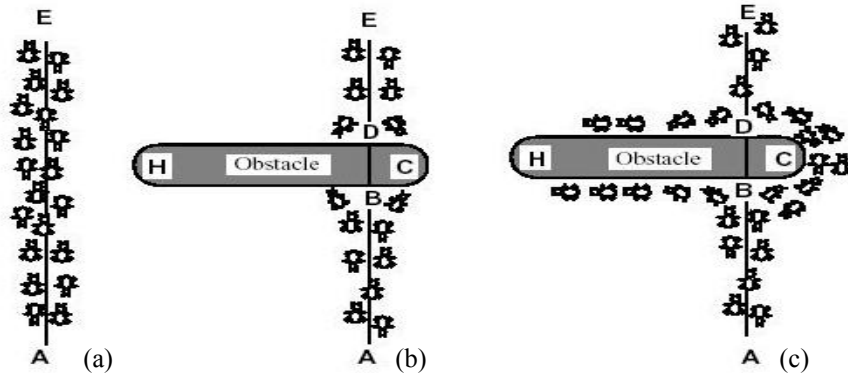

Figure 4. Paths followed by a group of ants from the nest (A) to the food source (E), [9]. (a) free path, (b) blockage caused by an obstacle, and (c) search for alternative paths with a concentration of ants on the shortest one (ABCDE).

The behavior of the ants represented schematically in Figure 4 is then used for the formulation and solution of an optimization problem.

In the ACS optimization method, several generations of ants are produced. For each generation, a fixed amount of ants (na) is evaluated. Each ant is associated to a feasible path that represents a candidate solution, being composed of a particular set of edges of the graph that contains all possible solutions. Figure 5 represents the discretization of the feasible range for each unknown. Here we consider that the range for each of the ns unknowns, τ_0, ω, ρ_1 and ρ_2, is discretized in $np = 128$ values. Each unknown is then depicted as a range of discretized values and is considered a node of the problem. Each ant consists on a set of edges that links a set of nodes (one for each unknown). Each edge is defined by a pair of randomly chosen values of the corresponding unknowns. Figure 5 also shows three ants, being each one composed by its own set of edges. Choosing the unknowns on a probabilistic basis generates each ant. This approach was successfully used for the Traveling Salesman Problem (TSP) and other graph like problems [2]. The best ant of each generation is then chosen and it is allowed to mark with pheromone its path. This will influence the creation of ants in further generations. The pheromone put by the ants decays according to an evaporation rate denoted by ϕ_{decay}. Finally, at the end of all generations, the best solution is assumed to be achieved. A solution (ant) is generated by linking the ns nodes by $(ns-1)$ edges. In order to connect each pair of nodes, np discrete values can be chosen. This approach was

developed in order to deal with real valued unknowns. In our inverse radiative transfer problem ns corresponds to the total number of unknowns, i.e. $ns = 4$, as shown in eqn. (2) and in Figure 5. All possible edges are represented by an array $[i, j]$ with $i = 1, 2, \ldots, ns$ and $j = 1, 2, \ldots, np$, being therefore $ns \times np$ possible edges available.

At the beginning of the algorithm, generation $k = 0$, all nodes of the array $[i, j]$ are assigned with the following concentration of pheromone $\phi_{ij}^{k=0} = \phi_0$. The amount ϕ_0 is calculated with a greedy heuristics, as suggested in [3], using an evaluation of the objective function $Q(\vec{Z})$ given by eqn. (3),

$$\phi_0 = \frac{1}{ns \times Q(\vec{Z}^*)} \tag{4}$$

As in the inverse problems we are not able to determine a priori a greedy heuristics, we decided to arbitrarily choose $\vec{Z}^* = \{\tau_0^*, \omega^*, \rho_1^*, \rho_2^*\}^{\mathrm{T}} = \{1, 1, 1, 1\}^{\mathrm{T}}$ in order to evaluate $Q(\vec{Z}^*)$ to be used in eqn. (4).

The best ant in a given generation is allowed to mark its path, i.e. its set of edges, with the maximum amount of pheromone, and this will have an influence on the choice of the ants in the following generation. Therefore, for the next generations, $k = 1, 2, \ldots$, the amount of pheromone for all nodes is given by

$$\phi_{ij}^k = (1 - \phi_{decay})\phi_{ij}^{k-1} + \delta_{ij,best}^{k-1}\,\phi_0 \tag{5}$$

where $\delta_{ij,best}^{k-1}$ is the Krönecker delta associated with the best ant in generation $k - 1$, i.e. the one who yields the lowest value for the objective function at the preceding generation $(k - 1)$.
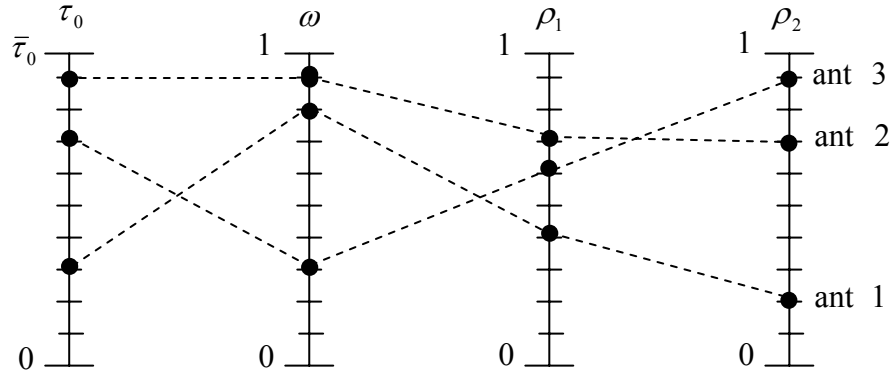

Figure 5. Schematical representation of the random generation of three ants.

The probability of a given edge $[i, j]$ to be chosen at generation k is given by [3,9]

$$P_{ij}^k = \frac{[\phi_{ij}^k]^\alpha [\eta_{ij}]^\beta}{\sum_{l=1}^{np} \{[\phi_{il}^k]^\alpha [\eta_{il}]^\beta\}} \tag{6}$$

where η_{ij} is the visibility/cost of each edge, a concept that arises from the TSP, where the cost is the inverse of the distance of a particular edge.

In eqn. (6) we assume that all edges are possible for any ant, but this is not the case for the TSP. The parameters α and β are weights used to establish a tradeoff between the influence of the pheromone and the visibility in the probability of choosing a given edge.

There is an additional scheme for the choice of an edge for a new ant. According to roulette, a random number in the range [0, 1] is generated for the new ant and it is compared with a parameter q_0 chosen for the problem. If the random number is greater than this parameter, the path is taken according to P_{ij} in eqn. (6). If not, the most marked edge is assigned.

In our inverse radiative transfer problem each ant corresponds to a candidate solution. The ranges of the unknowns are discretized according to $0 \leq \tau_0 \leq \bar{\tau}_0$ and $0 \leq \omega, \rho_1, \rho_2 \leq 1$. The radiative properties ω, ρ_1 and ρ_2 have physical meaning within the range [0,1], while τ_0 is mathematically unbounded in the upper limit. Nonetheless, in practical applications related to real inverse problem solution, we may consider an artificial

upper bound. Here we have considered $\bar{\tau}_0 = 1$. Note that for the calculation of ϕ_0 in eqn. (4) we have used the upper bounds for all the unknowns in $\vec{Z}^*$ in order to determine $Q(\vec{Z}^*)$.

In the present work we have not included any visibility information, η_{ij}. For instance, Preto *et al*. [16] considered the smoothness of the path as the visibility information for the estimation of the diffusion coefficient in a crystal growth inverse problem. The smoothness was then measured using Tikhonov's regularization terms [25].

The feasibility of including visibility information for the inverse radiative transfer problem will be investigated in future works. In such case, we will consider also the use of a regularization term in eqn. (3).

4. RESULTS AND DISCUSSION

4.1 Pure ACS minimization

As in most of stochastic optimization algorithms (and also deterministic algorithms), the quality of the solution obtained is related to the proper choice and fine tuning of the control parameters. For the ACS implementation performed in the present section we have considered: $\phi_{decay} = 0.03$ for the pheromone decay rate and $q_0 = 0.0$ for the parameter related to the choice of a new edge; this value implies that edges are chosen according to eqn. (6). In this equation, since visibility was not taken into account, the control parameters were taken as $\alpha = 1$ and $\beta = 0$.

We are interested in the estimation of the four unknown radiative properties given in eqn. (2). The range for each of the unknowns, already shown in the schematical representation given in Figure 5, is discretized into 128 values. Therefore, as explained in the previous section, $ns = 4$ and $np = 128$. A total of 200 generations $(mit = 200)$ are performed for each run of the ACS minimizer. At each iteration we consider a total number of $na = 128$ ants.

As real experimental data was not available, we generated synthetic experimental data by adding noise to the values calculated for the exit radiation intensities using the exact values of the radiative properties. In all test cases we have considered noiseless data as well as data with noise in the order of, or smaller than, 2% and 5%.

In order to evaluate the performance of the ACS minimizer we chose a relatively difficult test case with

$$\vec{Z}_{exact} = \{\tau_0, \omega, \rho_1, \rho_2\}^T = \{1.00, 0.50, 0.10, 0.95\} \tag{7}$$

The incident radiation was taken as $A_1 = 1.0$ and $A_2 = 0.0$ in eqns (1b) and (1c), respectively. The main difficulty for the solution of the inverse radiative transfer problem considered in this work is related to the estimation of ρ_1 since its effect will be sensed by the external detectors only after the radiation goes into the medium at $\tau = 0$, is reflected at $\tau = \tau_0$ and is then both transmitted and reflected at $\tau = 0$. This difficulty is confirmed by the sensitivity analysis related to this particular unknown.

For each set of experimental data (noiseless data, and 2% and 5% error noisy data) 10 different runs were performed, using different seeds for the random generation of the ants.

In Table 1 are presented the best, worst and average (for the 10 runs) estimated values for the radiative properties. From the second to the fifth columns of Table 1 are shown the exact and estimated values for τ_0, ω, ρ_1 and ρ_2, respectively. In the sixth column of Table 1 are given the values of the cost function, $Q(\vec{Z})$ defined by eqn. (3), and in the seventh column are presented the values for the square norm between the exact and estimated values for the radiative properties,

$$d^2 = \sum_{i=1}^{n_s} \left(\bar{Z}_{i_{exact}} - \bar{Z}_{i_{estimated}}\right)^2 \tag{8}$$

In order to assure convergence we have for convenience chosen a maximum number of 200 iterations (200 generations), but we have checked for each run the iteration in which convergence has been achieved (when no further change was observed in the values of $Q(\vec{Z})$ and d^2). This information is given in the last column of Table 1. As expected, the analysis of the results presented in Table 1 show that the poorest estimates are related to the unknown ρ_1.

In Figure 6 is shown, for one particular run of the ACS minimizer, the evolution of the cost function, $Q(\vec{Z})$, as well as the evolution of the deviation between the exact and estimated values of the radiative properties, d^2. In this particular run the set of noiseless data was considered. Similar behaviours were observed for the cases with noisy data. In Table 1 (as well as in Table 3) we observe that some results are repeated, i.e. the same ants appear in the test cases with different levels of noise in the experimental data.

The ACS algorithm is not completely random, since it is somewhat controlled by the probability of generating the ants in a generation according to the amount of pheromone in the previous generation. This is strongly influenced by the seed used for the generation of random numbers employed in the generation of the ants. The use of the same seed may yield solutions that are equal or similar in different test cases (noiseless data and 2% or 5% noisy data).

Table 1: Best, worst and average estimated values in 10 runs of the pure ACS minimizer, with 200 generations and 128 ants for each generation.

	τ_0	ω	ρ_1	ρ_2	$Q(\vec{Z})$, eqn. (3)	d^2, eqn. (8)	iteration
Noiseless data							
best (seed 21)[*]	1.0000	0.5000	0.1016	0.9531	1.30E-05	1.22E-05	98
worst (seed 75)	0.9531	0.5547	0.2891	0.9609	6.06E-05	4.11E-02	122
average (10 seeds)	0.9766	0.5274	0.1954	0.9570	1.03E-05	1.04E-02	110
Exact	1.00	0.50	0.10	0.95	0.00		
2% noisy data							
best (seed 21)	1.0000	0.5000	0.1016	0.9531	1.49E-05	1.22E-05	155
worst (seed 75)	0.9531	0.5547	0.2891	0.9609	6.16E-05	4.11E-02	122
average (10 seeds)	0.9766	0.5274	0.1954	0.9570	1.19E-05	1.04E-02	139
exact	1.00	0.50	0.10	0.95	4.55E-07		
5% noisy data							
best (seed 97)	1.0000	0.4922	0.0781	0.9453	2.34E-05	5.62E-04	149
worst (seed 75)	0.9531	0.5547	0.2891	0.9609	6.69E-05	4.11E-02	122
average (10 seeds)	0.9766	0.5235	0.1836	0.9531	1.10E-05	8.10E-03	136
exact	1.00	0.50	0.10	0.95	1.74E-06		

[*] The seeds used for the generation of the ants were chosen by randomly generating a real number in the range [0,1] and then scaling it up to the range [0,99] and picking the nearest integer.

We have observed that the ACS minimizer, or inverse solver, is computationally intensive. For each run with 200 generations, and 128 ants for each generation, a total of 25600 function evaluations is required, corresponding to about 17 minutes of CPU time on a AMD Athlon 1.67 GHz processor. We have used here a coarse mesh for the solution of the direct problem. If a typical finer mesh is used the CPU time goes up to 3 hours.
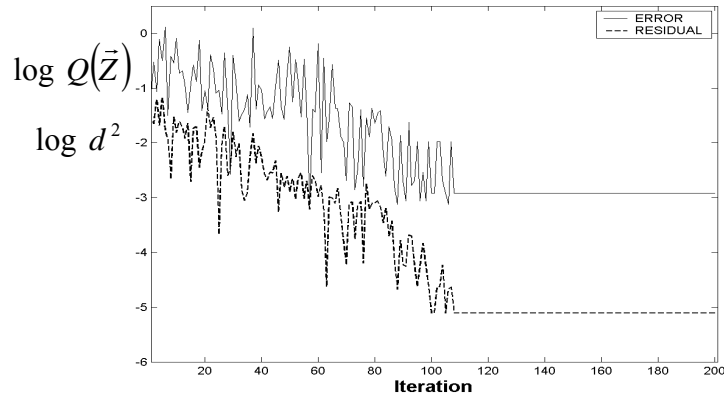

Figure 6. Evolution of the cost function, $Q(\vec{Z})$, and of the deviation between exact and estimated values of the radiative properties, d^2, for one run of the pure ACS minimizer with noiseless experimental data.

The most costly part of the algorithm is the evaluation of the ants, in which for each ant the solution of the direct problem given by eqns (1a-c) is required. Since the ants in each generation are totally independent, we noticed that the use of parallel computing could be quite effective, yielding high speed-up values and high efficiencies (close to 1). Therefore we have implemented a parallel version of the ACS minimizer using the MPI (Message Passing Interface) library [15] in order to execute it on a cluster of PCs.

In Table 2 are presented the results for the parallel implementation with p processors ranging from $p = 2$ to $p = 16$. We observe that the speed-up, $Su = T_s / T_p$ where T_s and T_p represent the times required for serial and parallel computation, respectively, is close to the ideal value, $Su \approx p$, as well as the efficiency, $E = Su / p$, that is $E \approx 1$.

Table 2: Execution time, speed-up and efficiency for the parallel implementation of the pure ACS minimizer.

Processors − p	Execution Time (s)	Speed-up, Su	Efficiency, E
1	999.22	—	—
2	501.43	1.99	1.00
4	250.45	3.99	1.00
8	125.76	7.95	0.99
16	63.63	15.70	0.98

4.2 Hybridization of ACS with the Levenberg – Marquardt method (ACS-LM)

By probing the search space (range of the unknowns) in a random way, a stochastic method, such as ACS, may lead to the vicinity of the global optimum, if it is properly implemented computationally. Nonetheless the computational effort is usually high.

Gradient based methods, such as the Levenberg-Marquardt method, are usually faster in their convergence, but they may get trapped in the closer local minimum.

Recently, hybrid approaches, coupling stochastic methods and the Levenberg-Marquardt method have been used successfully for the solution of inverse heat transfer problems of parameter estimation [20, 21]: SA-LM (Simulated Annealing and Levenberg-Marquardt) and GA-LM (Genetic Algorithms and Levenberg-Marquardt). Other hybrid strategies combining stochastic and deterministic methods have also been implemented [5].

In such hybrid approach the stochastic method (SA or GA) is run for a small number of individuals and generations (or cycles), requiring therefore a much smaller number of function evaluations. The solution obtained with the stochastic method is then used as the initial guess for the gradient based method. If necessary this approach may be iterated.

Artificial Neural Networks (ANN) have also been used for the same strategy of generating a good initial guess for the gradient based method: ANN-LM [22, 23].

Explicit and implicit formulations for the solution of inverse radiative transfer problems have also been combined in the same strategy [18, 19].

In the present work we have implemented the hybridization ACS-LM and the results will be presented next. The LM method will not be described here. Details may be found in [20, 21].

In this section, we considered the pure ACS minimizer described in Section 4.1, but now with only 25 generations ($mit = 25$), and only 16 ants ($na = 16$) in each generation, requiring a total of 400 function evaluations for each run of the ACS minimizer, which represents only 1.56% of the computational effort required in the previous section.

Other control parameters were also modified: 100 values for the discretization range of the unknowns, i. e. $np = 100$ and pheromone decay rate $\phi_{decay} = 0.30$.

In Table 3 are presented the best, worst and average estimated values for the radiative properties in 10 runs of the pure ACS minimizer. As shown in the last column of Table 3, all runs converged in less than 25 iterations. The ACS runs were also performed in parallel using the PC cluster with 16 processors.

The results obtained with the pure ACS minimizer, which are shown in Table 3, were then used as the initial guesses for the Levenberg-Marquardt method. The final results for such hybridization, ACS-LM, are shown in Table 4. The seventh column of the table shows the number of iterations required for the LM to converge within the tolerance of 10^{-5} in the deviation between two consecutive estimates for the radiative properties. In the last column of Table 4 it is shown the number of function evaluations (NFE) required for the convergence of the LM method.

Table 3: Best, worst and average estimated values in 10 runs of the pure ACS minimizer, with 25 generations and 16 ants for each generation. Each set of estimated values will be used as the initial guess for the LM method.

	τ_0	ω	ρ_1	ρ_2	$Q(\vec{Z})$, eqn. (3)	d^2, eqn. (8)	iteration
noiseless data							
best (seed 89)	0.84	0.61	0.46	0.95	1.62E-03	1.67E-01	20
worst (seed 97)	0.70	0.68	0.67	0.97	1.92E-03	4.48E-01	17
average (10 seeds)	0.77	0.65	0.57	0.96	1.34E-03	2.90E-01	19
exact	1.00	0.50	0.10	0.95	0.00		
2% noisy data							
best (seed 89)	0.84	0.61	0.46	0.95	1.64E-03	1.67E-01	20
worst (seed 97)	0.70	0.68	0.67	0.97	1.94E-03	4.48E-01	17
average (10 seeds)	0.77	0.65	0.57	0.96	1.35E-03	2.90E-01	19
exact	1.00	0.50	0.10	0.95	4.55E-07		
5% noisy data							
best (seed 89)	0.84	0.61	0.46	0.95	1.61E-03	1.67E-01	20
worst (seed 97)	0.70	0.68	0.67	0.97	1.92E-03	4.48E-01	17
average (10 seeds)	0.77	0.65	0.57	0.96	1.36E-03	2.90E-01	19
exact	1.00	0.50	0.10	0.95	1.74E-06		

From the results shown in Tables 1 and 4 it can be seen that both the pure ACS minimizer and the hybridization ACS-LM proved to be robust yielding good estimates for the radiative transfer properties, even for experimental data with noise. As expected the poorest results were observed for ρ_1 which is due to the lowest sensitivity of the experimental data with respect to this parameter.

Table 4: Results for the hybridization ACS-LM. The initial guesses for the LM method are shown in Table 3.

	τ_0	ω	ρ_1	ρ_2	$Q(\vec{Z})$, eqn. (3)	LM iter.	NFE[1]
Noiseless data							
best (seed 89)	0.999770	0.500368	0.101310	0.950050	9.88E-10	28	33
worst (seed 97)	0.999685	0.500538	0.101891	0.950072	2.47E-09	35	44
average	0.999728	0.500453	0.101601	0.950061	4.23E-10	19	24
Exact	1.000000	0.500000	0.100000	0.950000	0		
2% noisy data							
best (seed 89)	0.999299	0.501001	0.104053	0.949981	3.14E-07	25	30
worst (seed 97)	0.999417	0.500820	0.103418	0.949957	3.11E-07	29	46
average	0.999358	0.500911	0.103736	0.949969	3.12E-07	18	25
Exact	1.000000	0.500000	0.100000	0.950000	4.55E-07		
5% noisy data							
best (seed 89)	0.999443	0.502393	0.107760	0.949900	1.43E-06	21	30
worst (seed 97)	0.996418	0.508108	0.127230	0.950642	1.81E-06	34	50
average	0.997931	0.505251	0.117495	0.950271	1.43E-06	15	23
exact	1.000000	0.500000	0.100000	0.950000	1.74E-06		

[1]NFE ≡ Number of function evaluations

6. CONCLUSIONS

In the present work, both the Ant Colony System algorithm (ACS) and the hybridization of such method with the gradient based Levenberg-Marquardt method, ACS-LM, yielded good estimates for the radiative properties of a one-dimensional participating medium using the measured data of the intensity of the radiation acquired only by external detectors.

In future works we intend to compare the performance of the method with other stochastic methods.

Acknowledgements

REFERENCES

1. S. R. Arridge, Optical tomography in medical imaging. *Inverse Probl.* (1999) **15**, R41-R93.

2. J. C. Becceneri and A. S. I. Zinober, Extraction of energy in a nuclear reactor by ants, *Proceedings of the Brazilian Symposium on Operations Research,* Campos do Jordão, Brazil, 6-9 November, 2001.

3. E. Bonabeau, M. Dorigo and G. Theraulaz, *Swarm Intelligence: From Natural to Artificial Systems*, Oxford University Press, New York, 1999.

4. H. F. Campos Velho, M. T. Vilhena, M. R. Retamoso and R. P. Pazos, An application of the LTS_N method on an inverse problem in hydrologic optics. *Prog. Nucl. Energy* (2003) **42**, 457-468.

5. H. F. Campos Velho, F. M. Ramos, E. S. Chalhoub, S. Stephany S., J. C. Carvalho and F. L. Souza, Inverse problems in space science and technology, *Proceedings of the 5th International Conference on Industrial and Applied Mathematics - ICIAM*, Sidney, Australia, 7-11 July, 2003.

6. S. Chandrasekhar, *Radiative Transfer*, Dover Publications, Inc., New York, 1960.

7. A. Chedin, S. Serrar, A. Hollingsworth, R. Armante and N. A. Scott, Detecting annual and seasonal variations of CO_2, CO and N_2O from a multi-year collocated satellite-radiosonde data-set using the new rapid radiance reconstruction (3R-N) model. *J Quant. Spectrosc. Radiat. Transfer* (2003) **77**, 285-299.

8. I. J. D. Craig and J. C. Brown, *Inverse Problems in Astronomy: A Guide to Inversion Strategies for Remotely Sensed Data*, Adam Hilger Ltd., Bristol, 1986.

9. M. Dorigo, V. Maniezzo and A. Colorni, The ant system: optimization by a colony of cooperating agents. *IEEE Trans. Syst. Man. Cy. B* (1996) **26** (2), 29–41.

10. F. Gao, H. Niu, H. Zhao and H. Zhang, The forward and inverse models in time-resolved optical tomography imaging and their finite-element method solutions. *Image Vision Comput.* (1998) **16**, 703-712.

11. A. H. Hakim and N. J. McCormick, Ocean optics estimation for absorption, backscattering, and phase function parameters. *Appl. Optics* (2003) **42**, 931–938.

12. E. J. Hochberg, M. J. Atkinson and S. Andréfouët, Spectral reflectance of coral reef bottom-types worldwide and implications for coral reef remote sensing. *Remote Sens. Environ.* (2003) **85**, 159-173.

13. C. Miesch, F. Cabot, X. Briottet and P. Henry, Assimilation method to derive spectral ground reflectance of desert sites from satellite datasets. *Remote Sens. Environ.* (2003) **87**, 359-370.

14. M. N. Özisik, *Radiative Transfer and Interactions with Conduction and Convection*, John Wiley, New York, 1973.

15. P. Pacheco, *Parallel Programming with MPI*, Morgan Kaufmann Publishers, San Franscisco, 1997.

16. A. J. Preto, H. F. Campos Velho, J. C. Becceneri, M. Fabbri, N. N. Arai, R. P. Souto and S. Stephany, A new regularization technique for an ant-colony based inverse solver applied to a crystal growth problem, *13th Inverse Problems in Engineering Seminar (IPES-2004)*, Cincinnati, USA, 14-15 June, 2004, pp. 147-153.

17. C. E. Siewert, Inverse solutions to radiative-transfer problems based on the binomial or the Henyey-Greenstein scattering law. *J Quant. Spectrosc. Radiat. Transfer* (2002) **72**, 827-835.

18. A. J. Silva Neto, Explicit and implicit formulations for inverse radiative transfer problems, *5th World Congress on Computational Mechanics, Mini-Symposium MS 125 – Computational Treatment of Inverse Problems in Mechanics*, Vienna, Austria, 7-12 July, 2002.

19. A. J. Silva Neto and N. J. McCormick, An explicit formulation based on the moments of the exit radiation intensity for the one-dimensional inverse radiative transfer problem, *4th International Conference on Inverse

Problems in Engineering: Theory and Practice (4ICIPE), Angra dos Reis, Brazil, 26-31 May, 2002, **II**, pp. 347–354.

20. A. J. Silva Neto and F. J. C. P. Soeiro, Estimation of phase function of anisotropic scattering with a combination of gradient based and stochastic global optimization methods, *5th World Congress on Computational Mechanics*, Vienna, Austria, 7-12 July, 2002.

21. A. J. Silva Neto and F. J. C. P. Soeiro, Solution of implicitly formulated inverse heat transfer problems with hybrid methods, *Mini – Symposium Inverse Problems from Thermal / Fluids and Solid Mechanics Application – 2nd MIT Conference on Computational Fluid and Solid Mechanics*, Cambridge, USA, 17-20 June, 2003.

22. F. J. C. P. Soeiro, P. O. Soares and A. J. Silva Neto, Solution of inverse radiative transfer problems with artificial neural networks and hybrid methods, *13th Inverse Problems in Engineering Seminar (IPES 2004)*, Cincinnati, USA, 14-15 June, 2004, pp. 163–169.

23. F. J. C. P. Soeiro, P. O. Soares, H. F. Campos Velho and A. J. Silva Neto, Using neural networks to obtain initial estimates for the solution of inverse heat transfer problems, *Inverse Problems, Design and Optimization Symposium*, Rio de Janeiro, Brazil, 17-19 March, 2004.

24. R. P. Souto, H. F. C. Velho, S. Stephany and S. Sandri, Reconstruction of chlorophyll concentration profile in offshore ocean water using ant colony system, *First Hybrid Metaheuristics (HM-2004)*, Valencia, Spain, 22-23 August, 2004, pp. 19-24.

25. A. N. Tikhonov and V. S. Arsenin *Solutions of Ill-Posed Problems*. Winston and Sons, Washington, 1977.

26. H.-C. Zhou, Y.-B. Hou, D.-L. Chen and C.-G. Zheng, An inverse radiative transfer problem of simultaneously estimating profiles of temperature and radiative parameters from boundary intensity and temperature measurements. *J. Quant. Spectrosc. Radiat. Transfer* (2002) **74**, 605-620.